Supporting Information

Fixation and Permeabilization Approaches for Scanning Electrochemical Microscopy of Living Cells

Alexandra Bondarenko,* Tzu-En Lin, Petar Stupar, Andreas Lesch, Fernando Cortés-Salazar, Hubert Girault, Horst Pick,*

***Corresponding Authors**
E-mail: alexandra.bondarenko@epfl.ch. Tel.: +41 21 69 33144. Fax: +41-21-693-3667.
E-mail: horst.pick@epfl.ch. Tel.: +41 21 69 33132. Fax: +41-21-693-3667.

Table of Contents

SI-I. Chemicals

Ferrocene methanol (FcMeOH), ferrocene carboxylic acid (FcCOOH), 4-(2-hydroxyethyl)-1-piperazineethanesulfonic acid (HEPES), KH_2PO_4, K_2HPO_4, K_3IrCl_6, Na_2SO_4, $MgSO_4$, K_2SO_4, citric acid, Triton X-100, bovine serum albumin (BSA), TyR (from mushroom, ≥ 1000 unit/mg), 3,3',5,5'-tetramethylbenzidine (TMB), and hydrogen peroxide (3 % in PBS) were purchased from Sigma – Aldrich (Schnelldorf, Switzerland). Formaldehyde solution (4% in PBS) was from AlfaAesar (Karlsruhe, Germany). Anti-TyR monoclonal Abs T311 were obtained from BIO MEDICAL LLC., USA. Secondary anti-mouse Abs conjugated with HRP (Abs-HRP) were from Abcam (Cambridge, UK). Deionized water was produced by a Milli-Q plus 185 model from Millipore (Zug, Switzerland) and was used for all experimental solutions. Polyvinylidene fluoride (PVDF) membranes for protein blotting were purchased from Bio-Rad (Hercules, CA, USA).

The SECM experimental buffer was 10 mM HEPES pH 7.4, containing 75 mM Na_2SO_4, 1 mM $MgSO_4$ and 3 mM K_2SO_4. The PBS buffer (10 mM, pH 7.4) was containing NaCl 137 mM, KCl 2.7 mM, Na_2HPO_4 10 mM, KH_2PO_4 1.8 mM. As sample, washing and blocking buffers 1 % BSA in PBS and as a permeabilization buffer – 1 % Triton X-100 in PBS were used. The substrate solution was 0.2 mM TMB and 0.1 mM H_2O_2 mixture in 0.1 M citrate-phosphate buffer, pH = 5.0.

Human melanoma cell lines WM-239, WM-115, and Sbcl2 as well as cervical cancer HeLa and breast cancer MCF7 cells were purchased from the American Type Culture Collection (ATCC) and cultured in Dulbecco's modified Eagle's medium (Gibco Life Technologies), supplemented with 10% fetal calf serum (FCS) at 37 °C in humidified atmosphere with 5% CO_2. 24 hours before each experiment, 10 µL of cells suspension were plated on non-treated glass slides within the three chambers of a specifically prepared polyimide (PI) mask for cell patterning. After the cells were attached to the surface, the glass slides were placed in cell culture dishes (35 mm × 10 mm, Nunc, Denmark) filled with the Eagle's medium. The PI mask was removed directly before the SECM experiments and the glass slides were positioned within the electrochemical cell filled with the experimental buffer. The optical control of the cultured cells was performed before and after SECM experiments by using a laser scanning microscope (VK8700, Keyence).

Additionally, in order to facilitate the UME positioning, after the optical confirmation of the cells being in a good state and distributed uniformly within the chamber, the glass on the opposite side from cells was marked using a thin marker. Thus, when the glass with cells was positioned on the SECM setup, it was possible to position the electrode above the area of interest. Finally, in order to position the UME exactly above the cell of interest (i.e. when the approach curves toward cells were performed), the sample was placed above a hole at the SECM tilt table and the cell surface-UME positioning was observed and aligned with a Proscope camera that was fixed under the table.

The intracellular TyR immunostaining was based on the fixation/permeabilization protocols combined with an immuno-histochemistry (IHC) procedure. Briefly, fixed and permeabilized cells were placed into 3% H_2O_2 solution for 15 min at RT in order to block the possible endogenous peroxidase activity. Thereafter, the sample was washed 5 times with PBS and then incubated in the blocking buffer for 30 min. In the next step, the glass slide with adherent cells was transferred into the solution of primary Abs (dilution 1 to 50 in the load-ing buffer), kept for 1 h at RT and washed 5 times with the washing buffer. Then the sample was incubated for 1 h with Abs-HRP (dilution 1 to 20000 in the sample buffer), washed 5 times with washing buffer and transferred into the electro-chemical cell filled with substrate solution. The presence of TyR was established by electrochemical detection of the en-zymatically produced 3,3',5,5'-Tetramethylbenzidine diimine (TMB_{ox}) at the scanning microelectrode (SECM details vide infra). In order to investigate the presence of Abs-HRP non-specific binding the above protocol was carried out, but with-out the incubation step with anti-TyR Abs.

SI-II. Preparation of the polyimide (PI) masks

Disposable PI masks with three parallel chambers for cell patterning were made of 125 μm-thick PI films (Kapton HN®; Goodfellow, Huntingdon, England). The PI sheet was fixed on one side of a double side tape (model 4959; Tesa SE, Beiersdorf Company). Thereafter, three parallel rectangles, 1 mm wide, 10 mm long and separated by 1 mm, were carved into a 10 mm wide and 20 mm long PI sheet by using a cutter-plotter (RoboPro CE5000-40-CRP, Graphtec Corporation, USA). The obtained PI masks were sterilized with ethanol and placed on a sterile microscopic glass slide for cell culturing.

SI-III. SECM of alive, fixed and permeabilized cells. Theory

SECM is a type of scanning probe microscopy (SPM) widely applied for characterization of various substrates topography and reactivity. It is based on recording the current at an ultramicroelectrode (UME), which is positioned or scanned in a proximity to a substrate in the presence of an electrolyte solution. The current, detected at the UME is a function of the tip-substrate distance *d* and the electrochemical activity of the surface. Thus, when the UME is approached towards an insulating or not electrochemically active substrate, it will simply block the diffusion of the redox mediator towards the UME (Figure S1a) and as result the tip current will decrease due to the depletion of the redox mediator' concentration within the UME-substrate gap (i.e. negative feedback). In contrast, if the substrate is conductive or electrochemically active, the regeneration of the redox mediator at the substrate can take place (Figure S1b) and as a result, the tip current will increase due to the increase of the redox mediator's concentration within the UME-substrate gap (i.e. positive feedback). [1]

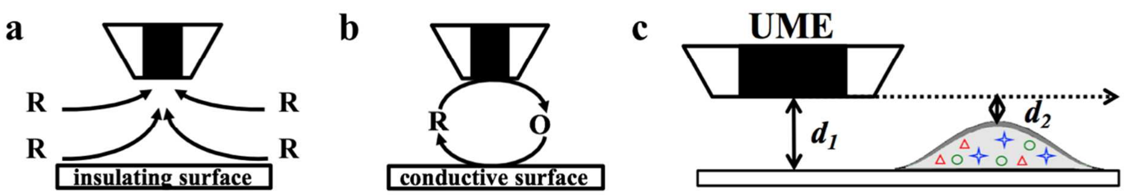

Figure S1. Schematic representation of the situations leading to negative (a) and positive (b) feedback in SECM and the influence of cell topography during the line scan above adherent cells (c).

Furthermore, during a horizontal line scan above the adherent cells, the tip-substrate distance is changing due to the cell topography (Figure S1c, $d_2 < d_1$). Thus, if the cell is non-electrochemically active and it does not permeate the redox mediator, a significant current decrease will be detected at the UME. In contrast, if the cell is electrochemically active and can regenerate the redox mediator, the detected current will increase. Unfortunately, the presence of various cellular processes (e.g. transmembrane transport) and low electrochemical activity of cells make difficult the interpretation of the recorded signal, especially in case if a hydrophobic redox mediator is employed.

Previously published SECM investigations of living cells presented the ability of hydrophobic and hydrophilic redox mediators to cross through the cell membrane.[11,12] In the present work, FcMeOH and FcCOOH were employed as a hydrophobic and hydrophilic redox mediators, respectively. For instance, FcMeOH can penetrate into the intracellular space spontaneously (*i.e.* passive transmembrane transport) and become an indicator of the intracellular biological electrochemical activity. In contrast, FcCOOH can only penetrate inside cells if an active transmembrane transport occurs and in its absence only cells topography will be recorded by SECM. In case of formaldehyde cells fixation, only passive transport of the redox mediator through the cells' membrane should occur. As a result, there will be no opportunity for FcCOOH to penetrate into cells and only cell topography information can be extracted by SECM. In the same time, cells will stay permeable for FcMeOH and the current recorded at UME will represent both passive transmembrane transport and cell topography. Additionally, cell membrane permeabilization will open access to the intracellular space for any compound independent on its hydrophilic properties (Figure S2).

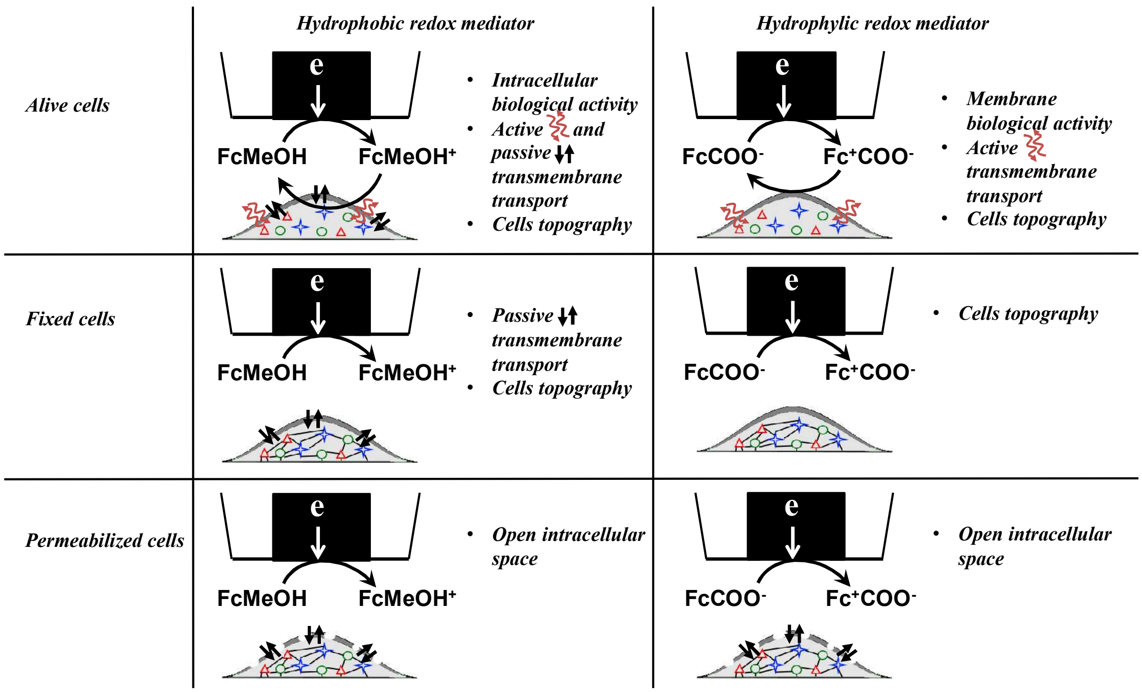

Figure S2. Schematic representation of the different type of information that can be extracted based on the type of redox mediator employed and the cells state (*i.e.* alive, fixed and permeabilized).

SI-IV. Influence of cell density on SECM signal

In order to investigate the influence of the cells population on the SECM signal, WM-115 cells were seeded at 3 different concentrations. The optical images of the obtained cell surfaces are presented in Figures S2 a – c. As it can be seen, serial dilution of the initial cells culture led to a significant difference in the obtained cell surface coverage, *i.e.* population within line 1 (Figure S3a) < line 2 (Figure S3b) < line 3 (Figure S3c).

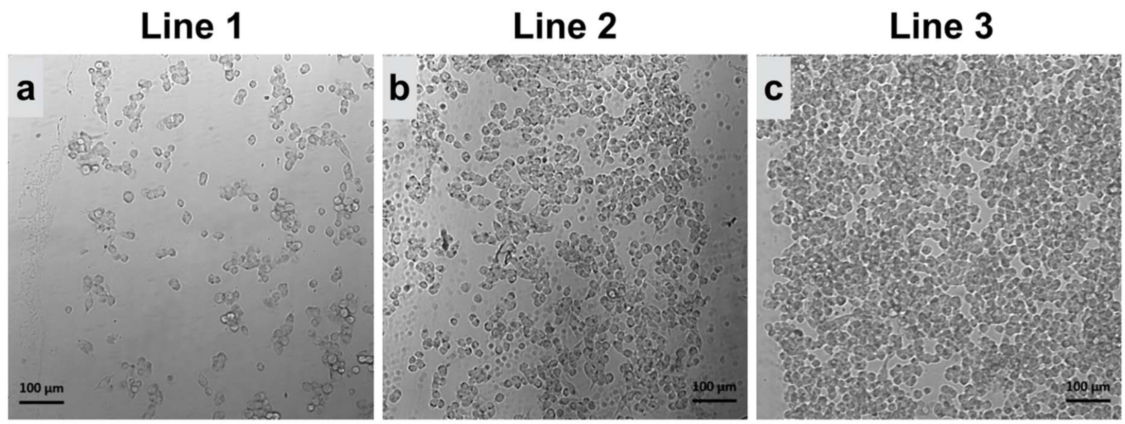

Figure S3. Optical images of fixed WM-115 cells at different cell populations (a) – (c). Cell surfaces (a), (b) and (c) were obtained by seeding melanoma cells with concentrations C3, C2 and C1 respectively, where 9×C3 = 3×C2 = C1 = 5×10^5 cells/mL

SI-V. Topographical changes of cells during fixation / permeabilization approach

Figure S2 represents the same cell surface when cells are alive (Figure S4a), fixed (Figure S4b) and permeabilized (Figure S4c). As a result, no significant morphological changes were observed. For instance, the cell marked in Figure S3a had a diameter equal to 22 μm, which stayed constant during all the manipulations (Figure S4b and c). These results are in good agreement with the ones reported before, where no influence of cross-linking agents on cells height was reported by AFM.[4]

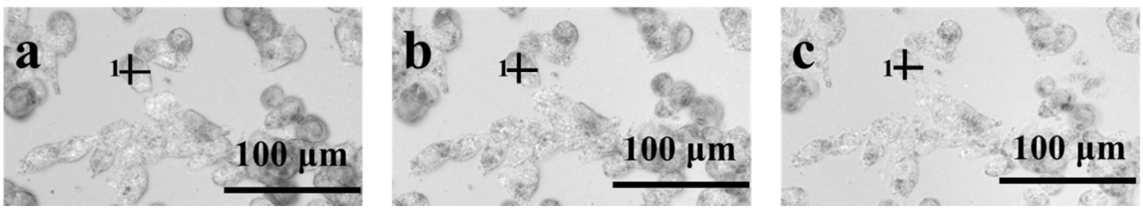

Figure S4. Optical images of alive (a), fixed (b) and permeabilized (c) adherent WM-115 cells.

Atomic Force Microscopy (AFM) measurements were made using Nanowizard III AFM from JPK Instruments (Berlin, Germany), coupled with a Zeiss Axiovert inverted optical microscope. A liquid exchanging system has been incorporated, capable of replacing the incubation medium during measurements with no effect on the image acquisition. Images were collected using Shocon (AppNano) cantilevers, with a nominal spring constant of 0.14 N/m. Quantitative imaging mode has been used. JPK's processing software and Gwyddion (v. 2.36) were used for flattening the images and no further image processing has been carried out.

In order to compare the topographical changes between alive and fixed cells, an AFM image of a WM-115 cell adherently grown on a Petri dish surface was investigated. Thus, on the first step the growing media was exchanged with the SECM experimental buffer and the image of alive cell was obtained. Thereafter, the solution was exchanged with the formaldehyde and incubated during 15 min. Further, the sample was washed 3 times with the experimental buffer and kept in it during AFM imaging of the same cell in a fixed state. On the last step a permeabiization buffer was added, the sample was washed 5 times and the AFM image of the cell in a permeabilized state in the experimental buffer was obtained. The resulting images (Figure S5) were obtained using "Facet Level" option in Gwyddion (http://gwyddion.net/documentation/user-guide-en/leveling-and-background.html). It levels data by subtracting a plane similarly to the standard "Plane Level" function, making facets of the surface as horizontal as possible.

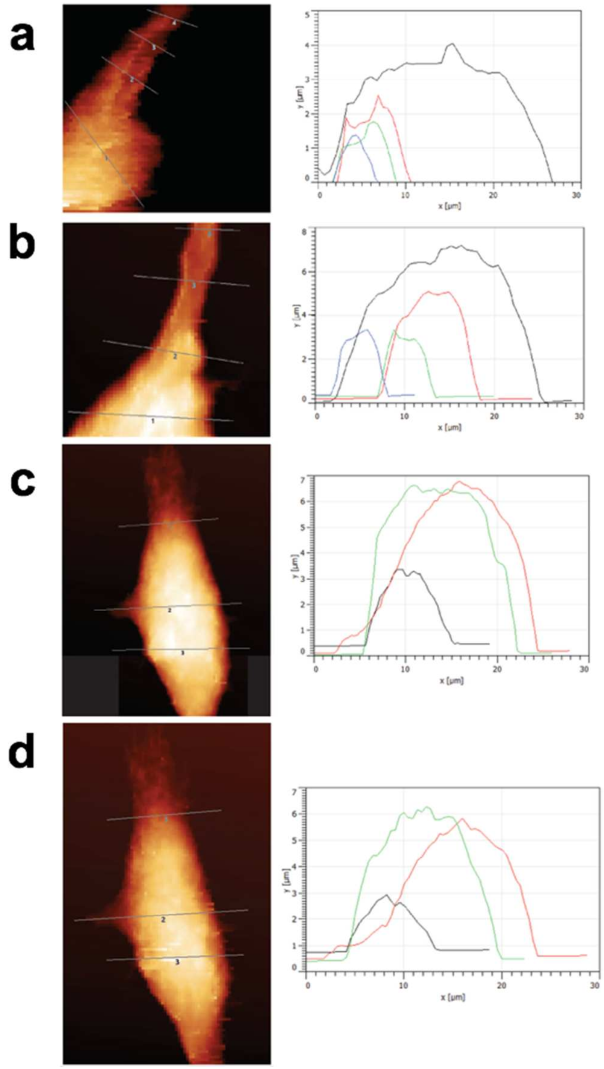

Figure S5. AFM image of two different WM-115 cells (left column) and the topography profile (right column) extracted from lines 1, 2, 3, and 4 (black, red, green and blue, respectively). One cell is representing differences between alive (a) and fixed (b) state, another one – between fixed (c) and permeabilized state (d).

Besides AFM, SECM approach curves towards cells in alive, fixed and permeabilized state were performed. On the first step, the sample surface was levelled using a tilt table based on approach curves over insulating and cell-free regions in the presence of the corresponding redox mediator (FcMeOH or FcCOOH). Thereafter, the probe was positioned on the distance equal to 100 μm above the surface and moved to the cell region. Further, the probe was approached towards the sample at the distance equal to 15 μm. The number of approach curves was collected at 3 different points above cells surface. The approach curves for cells in different states were carried out above the same points. The results of the experiments are presented in Figure S6.

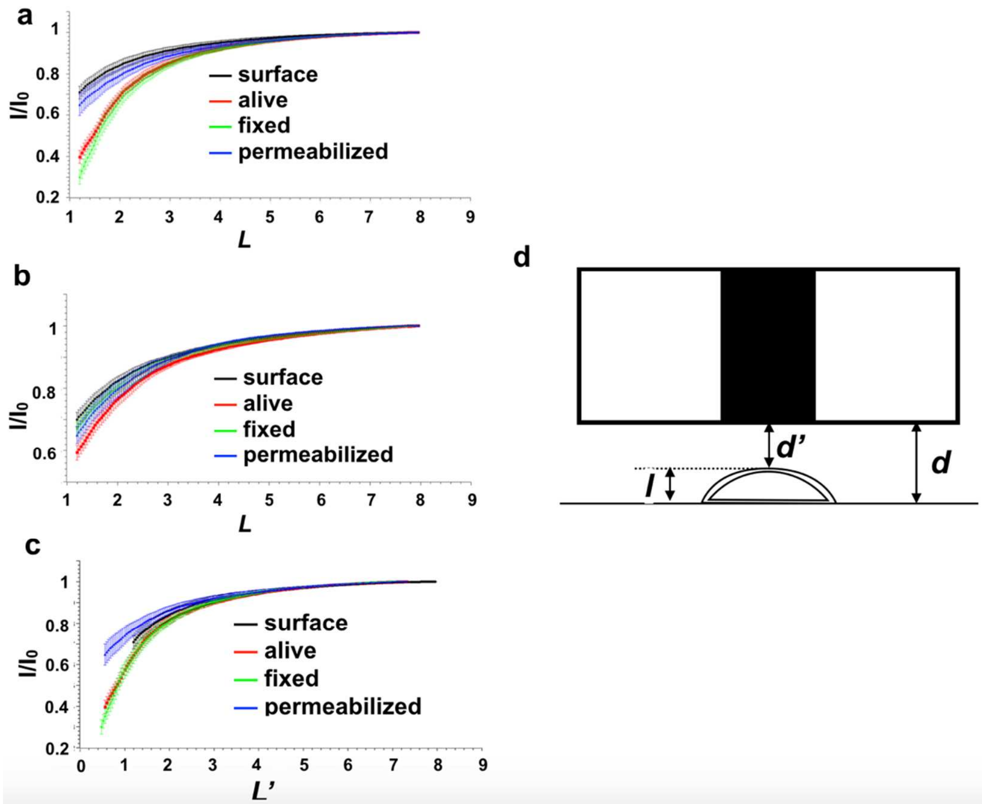

Figure S6. SECM approach curves towards cells in different states (i.e. alive, fixed and permeabilized) when FcCOOH (a)and (c) and FcMeOH (b) were employed as redox mediators. Schematic representation of UME positioned above cells (d).

The normalized approach curves presented in Figures S6a and S6b were plotted with the working distance *d* in respect to the insulating substrate surface. The cell topography has not been considered. However, since FcCOOH cannot penetrate inside cells, the real working distance between the cell surface and the UME (*d'*) will be smaller in comparison with the distance between the glass surface and the UME (*d*) due to the cell height (*l*) (*i.e. d'* is 5 – 7 µm smaller over the center a cell than *d*). In a normalized approach curve (Figure S6c), the normalized current is plotted versus the normalized working distance $L = d/r_T$, and $L' = d'/r_T$, where r_T is the radius of the Pt disk of the UME (Figure S6d).

SI-VI. SECM of alive, fixed and permeabilized cells. Experiments.

A)

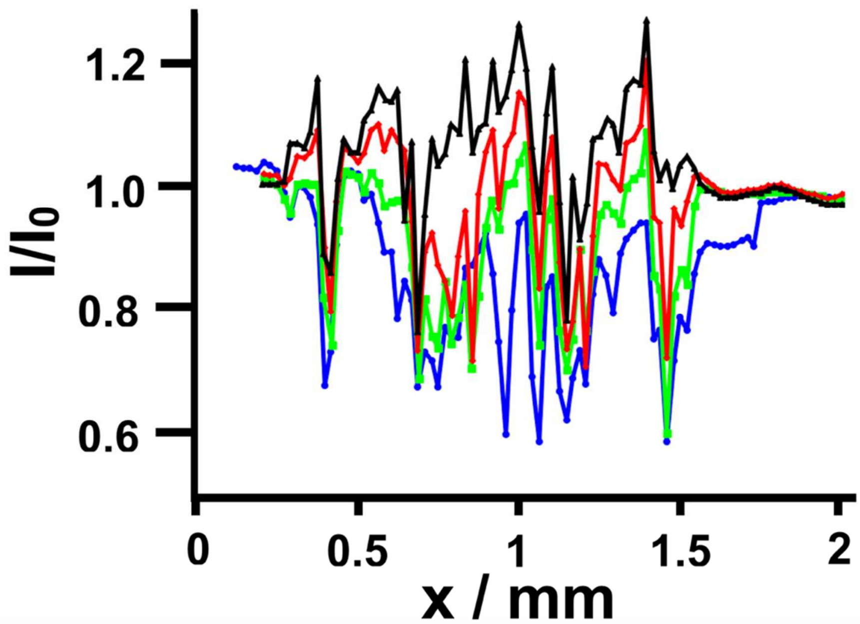

B)

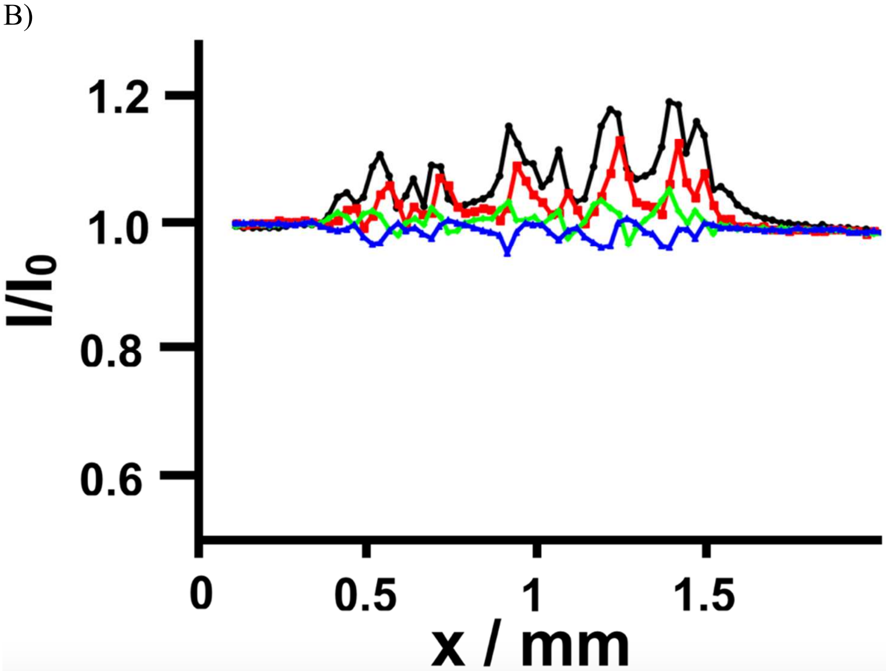

C)

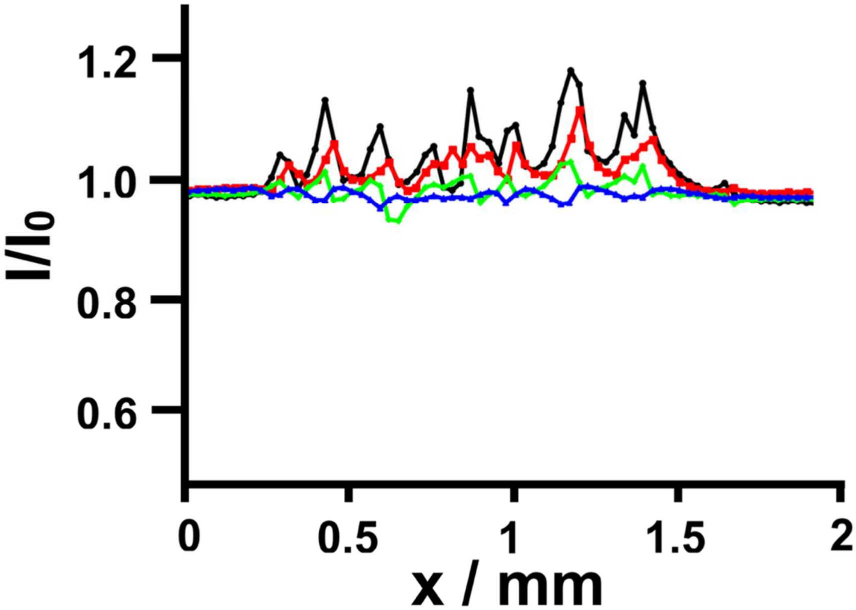

D)

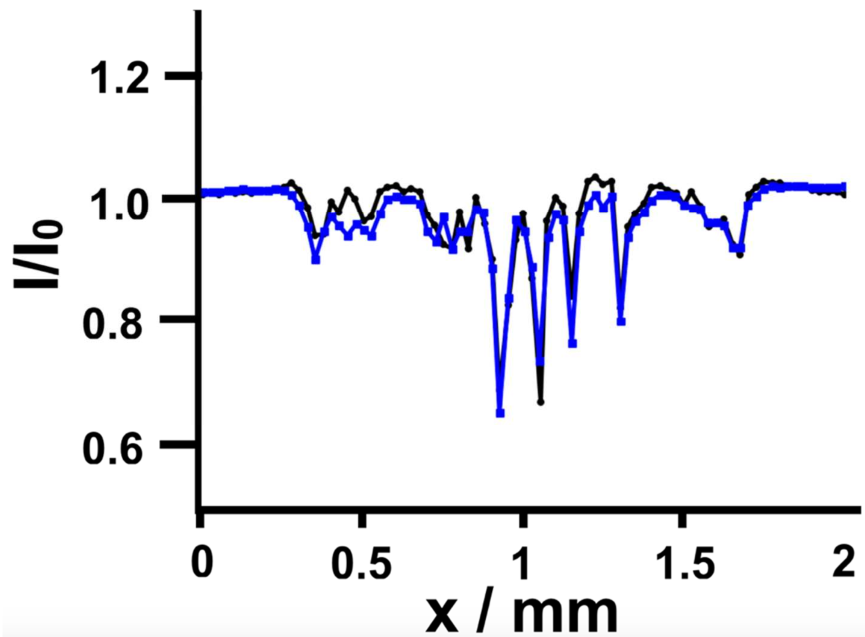

E)

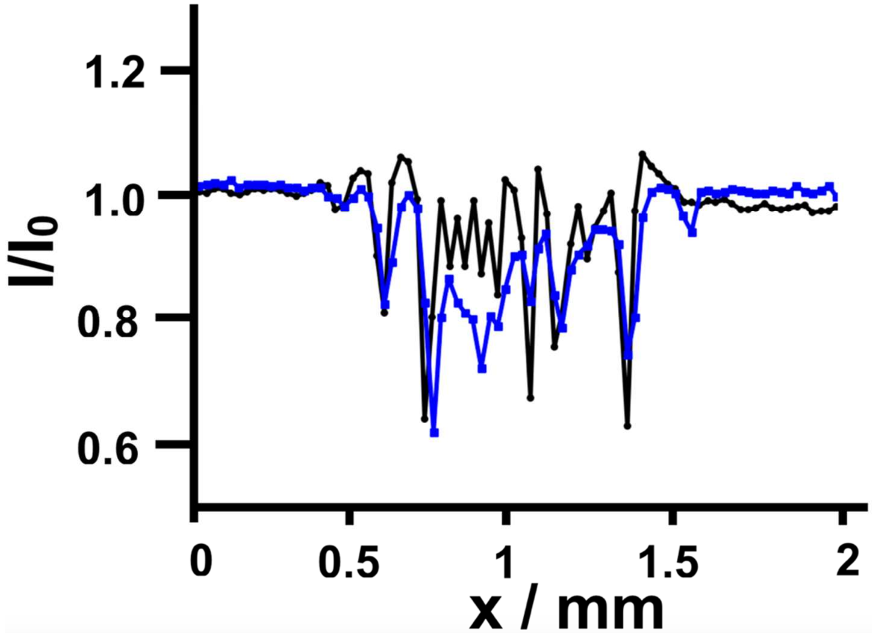

F)

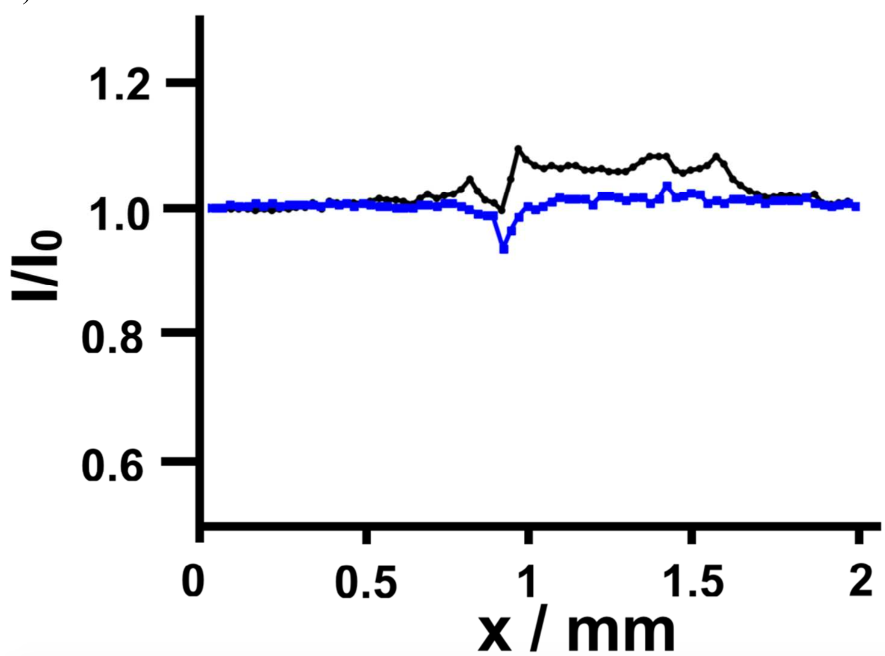

Figure S7. Influence of the UME translation speed on the SECM response (normalized current) provided by alive (a and d), fixed (b and e) and permeabilized (c and f) adherent WM-115 melanoma cells in presence of non-charged (FcMeOH, a – c) and charged (FcCOOH, d – f) redox mediators. 5 µm/s, 10 µm/s, 15 µm/s, 25 µm/s.

SI-VII. Inkjet-printed cell-like sample

To mimic the topography of cells and its influence on the recorded signal, several spots were prepared on polyethylene terephthalate sheets (PET; 125 µm thick; Goodfellow, UK) by inkjet printing of a dielectric material (*i.e.* UV curable ink JEMD6200, Sun Chemical, USA). An X-Serie CeraPrinter (Ceradrop, France) was equipped with a disposable, piezoelectric driven DMP cartridge (Dimatix Fujifilm, USA) containing 16 nozzles and providing a nominal droplet volume of 10 pL. During printing, the UV curable ink was polymerized by simultaneous UV light exposition. This was achieved by the UV LED FireEdge FE300 (380-420 nm; Phoseon Technology, USA) that was integrated into the printhead slot of the X-Serie printer and mounted slightly behind the DMP cartridge. All printing parameters, such as jetting frequency, waveform and number of active nozzles, were adjusted for optimum inkjet printing. The final patterns of insulating spots were made by printing three layers of 250 µm separated droplets. The printed patterns were investigated by laser scanning microscopy in a reflection mode.

The prepared sample contained several spots (30 µm diameter and approximately 6 µm height) positioned 250 µm from each other (Figure S8a – c), completely impermeable and inert to the redox mediators. The SECM images of the IJP sample using FcMeOH as the redox mediator at translation speeds equal to 5 µm/s and 25 µm/s are presented in Figures S8d and S8e, respectively. As expected, a clear decrease of the recorded current at the UME occurs when it is scanned over the dielectric spots for both translation speeds. However, when scanning at high translation rates a slight current increase is observed just before the drastically current decrease when the probe starts to scan the dielectric spot, which is similar to what was observed with alive and fixed cells.

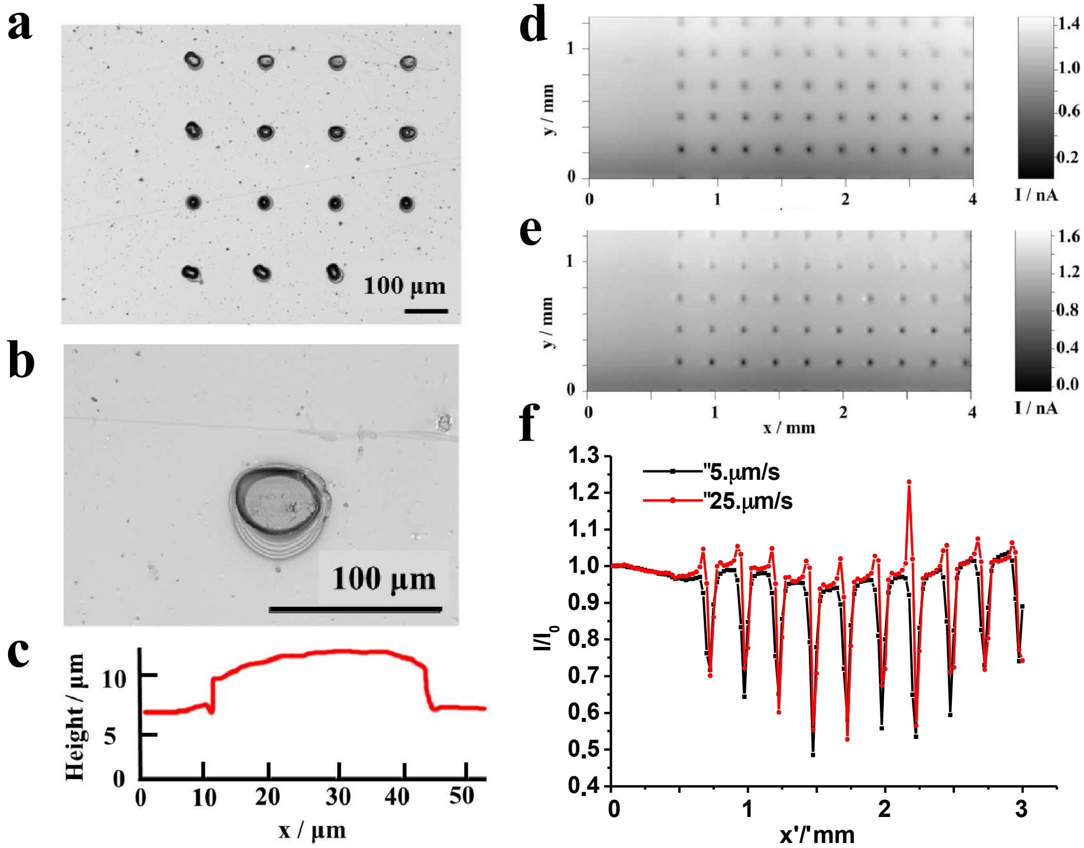

Figure S8. Optical images of the inkjet-printed UV-curable ink patterns (a) and (b) and the height profile of the pattern (c). 2D image (d) and (e) obtained with the translation rate 5 µm/s and 25 µm/s and the electrochemical signal (current) during SECM line scan (f) above the inkjet printed sample. Experimental conditions: working electrode – Pt UME (r_T = 12.5 µm, RG = 5), QRE – Ag, CE – Pt, the working distance d was equal to 15 µm, 0.1 mM FcMeOH in experimental buffer (pH = 7.4) was employed as the redox mediator

SI-VIII. SECM of proteins adsorbed on PVDF membrane

The immobilization of BSA and TyR on PVDF membrane was performed as it was described by *Lin at al*.[5] Briefly, the PVDF membrane was wetted by placing it in methanol (5 – 10 sec) and in deionized water (1 min), consequentially. Thereafter, 1 µL of each protein solution (10 mg/mL) was deposited on the membrane and dried under a gentle stream of nitrogen. The protein spots were separated by 1 – 2 mm of clean PVDF membrane. In the next step, the membrane was transferred into the electrochemical cell and leveled by using the oxygen reduction current obtained from oxygen diffusing out from the membrane pores.[5] Thereafter, Pt UME was translated over the protein spots at d = 25 µm with a translation rate equal to 25 µm/s. As a result, a clear current increase was observed when scanning above both proteins, especially at the edges of the protein spots due to the well-known “coffee ring” effect.

In order to better study possible height variations provided by spotting proteins on the PVDF membrane, the membrane with TyR spot was cut in 2 pieces as it is presented in the Figure a. Accordingly, Figure b represents the optical image of TyR spot, obtained with the laser microscope. Thereafter, the surface obtained after the cut (Figure S9c) was also studied under the microscope. As it can be seen from the Figure S9d, adsorbed proteins in the concentrations present in this article, do not induce any variation on the PVDF height.

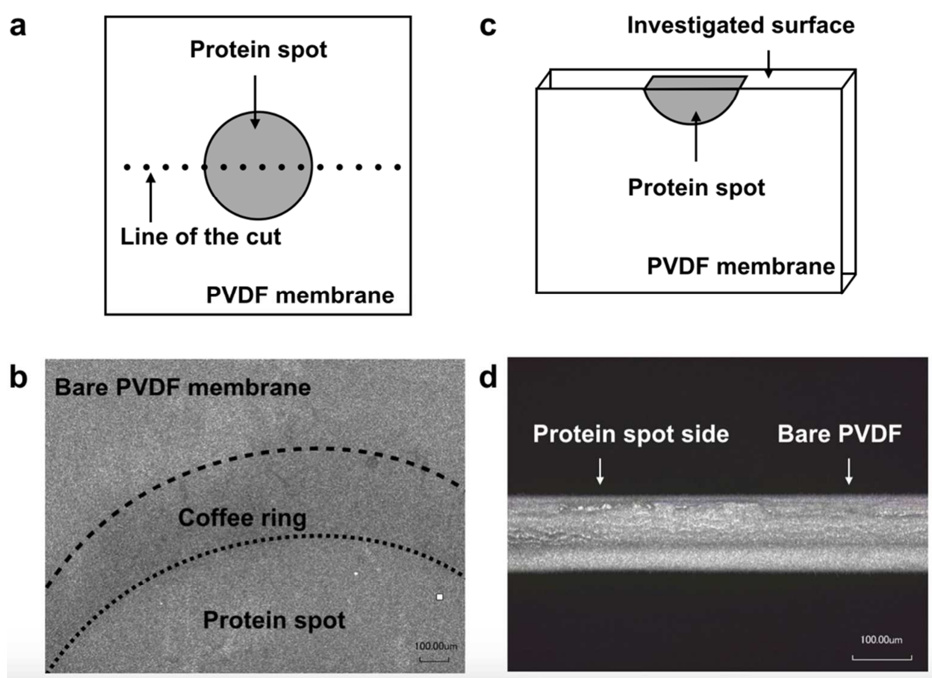

Figure S9. Schematic representation (a) and an optical image (b) of a protein spot on a PVDF membrane. Schematic representation of the PVDF membrane surface obtained after the cut (c) and its optical image (d).

SI-IX. SECM/immunostaining approach

After the immunostaining protocol was performed, the sample was placed on the SECM sample holder, levelled and then immersed into the substrate solution. Before starting the SECM experiments, the electrochemical behaviour of the employed UME was characterised by CV in presence of TMB. As it was expected, a sigmoidal electrochemical response corresponding to a two-electron transfer process was obtained with a relatively small capacitive current (Figure S10a).

In order to investigate the influence of cell topography on the detected electrochemical signal, fixed/permeabilized cells that have not been immunostained were scanned by using an UME located at a probe-substrate distance equal to 15 μm in presence of TMB (Figures S10b and c, green). Indeed, non-significant influence was observed on the SECM line scans due to the cells topography or intracellular reactivity, which suggests that under the experimental conditions SECM imaging of the immunostained intracellular TyR can be performed without any external interference.

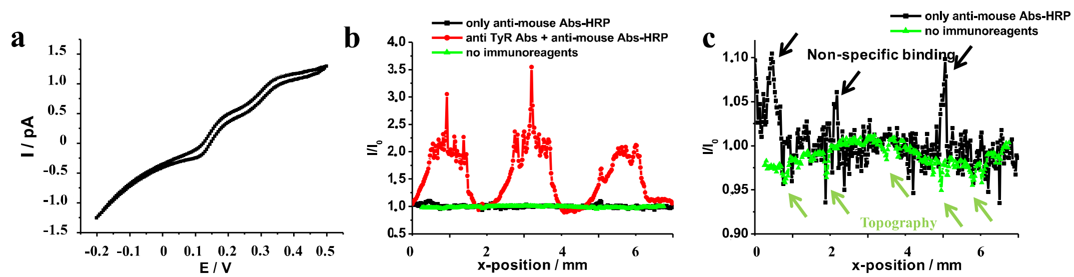

Figure S10. Cyclic voltammogram at a Pt UME in the presence of 0.2 mM of TMB and 0.1 mM of H_2O_2 solution (a) and line scans above WM-115 cells patterns with different cell density obtained by seeding cells at different concentrations (C1 = 5×10^5 cells/mL, C1 = 3×C2 = 9×C3) (b) and (c). The normalised current is presented for experiments where *i*) only Abs-HRP (b and c, black), *ii*) both primary anti-TyR Abs and secondary Abs-HRP (b, red) and *iii*) none of immunoreagents (b and c, green) were used. Experimental conditions: working electrode = Pt (r_T = 12.5 μm, RG = 5), QRE = Ag, CE = Pt. CV: performed at the bulk solution with a scan rate was equal to 25 mV/s. SECM: the working distance (*d*) was equal to 15 μm and the translation speed was equal to 25 μm/s. The normalisation of the current was performed on a signal recorded above the cells-free glass surface during the line scan.

To evaluate the non-specific binding of anti-mouse Abs-HRP on fixed and permeabilized cells, the fixed and permeabilized cells after blocking the surface with BSA were directly incubated with secondary Abs. The SECM line scans above cells presented a non-significant increase on the current (*i.e.* 5-10%) indicating that the signal coming from non-specific binding is negligible in comparison with the detected analytical current when specific TyR labelling was performed (Figure S10b and c). Additionally, when the full immunostainig procedure was performed, the increase of the working distance from 15 μm to 25 μm significantly decreases the resolution of the SECM image (Figure S11a and b). Working distances smaller than 15 µm were not tested due to the higher probability of probe-substrate crashes and the increase of the cells topographical component in the observed signal.

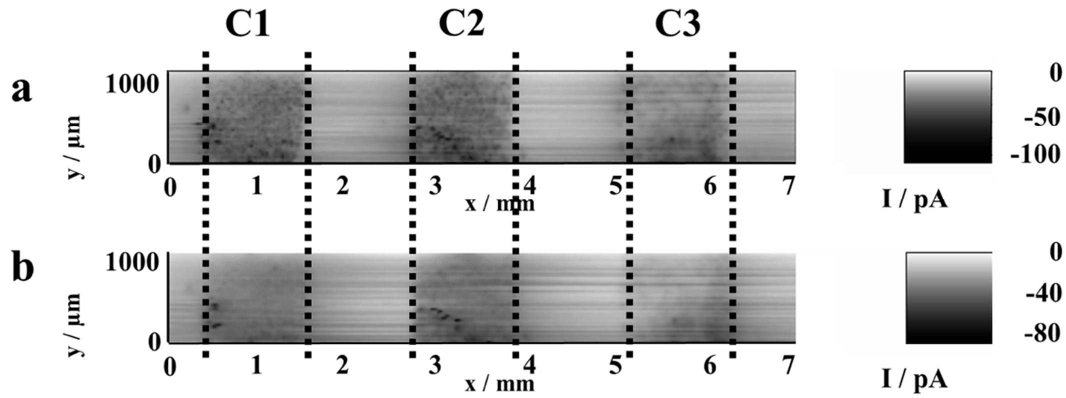

Figure S11. Investigation of TyR expression inside WM-115 cells by following immunostaining-SECM strategy. The adherent cells were grown at different density (C1 = 5×10^5 cells/mL, C1 = C2*3 = C3*9). Experimental conditions: working electrode = Pt (r_T = 12.5 µm, RG = 5), working distance = 15 µm (a) and 25 µm (b), the translation speed was equal to 25 µm/s and the substrate solution was containing 0.2 mM of TMB and 0.1 mM of H_2O_2.

SI-X. Data extraction from the SECM image of intracellular TyR (Figure 4)

The currents were extracted every 0.1 mm in y direction from every data point as it is presented in Figure S12.

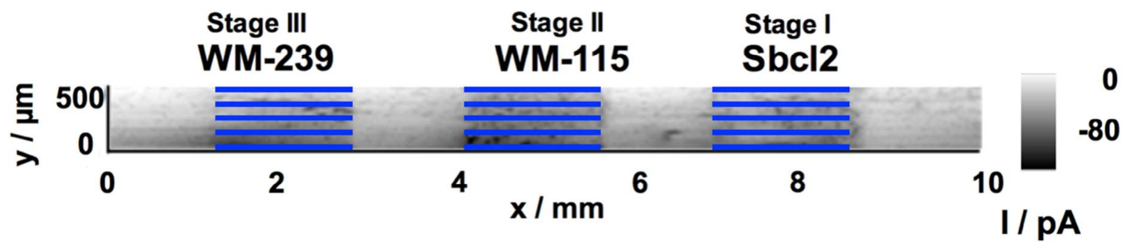

Figure S12. Illustration of the data extraction points, used to calculate the average value for each cell line

References

1 A. J. Bard and M. V. Mirkin, *Scanning Electrochemical Microscopy*, CRC Press: Boca Raton, second., 2012.

2 T. Yasukawa, I. Uchida and T. Matsue, *Biochim. Biophys. Acta*, 1998, **1369**, 152–158.

3 S. Amemiya, J. Guo, H. Xiong and D. A. Gross, *Anal. Bioanal. Chem.*, 2006, **386**, 458–471.

4 Y. Yamane, H. Shiga, H. Haga, K. Kawabata, K. Abe and E. Ito, *J. Electron Microsc. (Tokyo).*, 2000, **49**, 463–471.

5 T.-E. Lin, F. Cortés-Salazar, A. Lesch, L. Qiao, A. Bondarenko and H. H. Girault, *Electrochim. Acta*, 2015, **179**, 57–64.